Improving the Performance of Broadband Indoor MIMO PLC Systems by Combining Interference Alignment and Noise Whitening

Javier Giménez, José A. Cortés and Luis Díez
Communications and Signal Processing Lab.
Telecommunication Research Institute (TELMA), Universidad de Málaga
E.T.S.I. Telecomunicación, 29010 Málaga, Spain.
email: {javierg, jaca, diez}@ic.uma.es

Lutz Lampe
Department of Electrical and Computer Engineering
The University of British Columbia
Vancouver, BC V6T 1Z4, Canada.
email: lampe@ece.ubc.ca

***Abstract*—Interference alignment (IA) improves the sum rate of indoor broadband multiple input multiple output (MIMO) power line communications (PLC) systems in multi-user scenarios by allowing simultaneous connections over the shared medium. Similarly, the data rate can be enhanced by exploiting noise correlation by means of a whitening transformation. This work assesses the performance gain achieved by combining IA and noise whitening (NW) in MIMO PLC multi-user scenarios. Since NW renders the equivalent channel non-reciprocal and most IA algorithms are based on this assumption, a novel IA algorithm that does not rely on this property is proposed. The presented analysis takes into account the overhead of the feedback of the channel state information (CSI) required by the IA scheme. The assessment is accomplished in a set of 1000 scenarios generated out of measured channels. Obtained results show that the proposal improves the sum rate in the 2–88 MHz band by 95.6 Mbit/s in the 20th percentile, and 50 Mbit/s in the 80th percentile. While in the 88–108 MHz band absolute gains are smaller because the low power spectral density (PSD) of the injected signal, relative gains exceed 20% in 40% of the scenarios.**

I. Introduction

Indoor broadband power line communications (PLC) is a mature technology for delivering multimedia content in homes and small offices, where it can also cooperate with wireless systems to improve coverage. It has also been proposed as a backhaul for visible light communications (VLC) and Internet of things (IoT) applications [1] [2]. The ITU-T G.hn standard and the Homeplug AV2 industry specification define two of the most widely used systems in these contexts [3] [4] [5]. They employ multiple input multiple output (MIMO) orthogonal frequency division multiplexing (OFDM)-based systems with 4096 subcarriers in the frequency band up to 100 MHz.

The referred PLC systems avoid multi-user interference by using time-division multiple access (TDMA) with both contention-free and carrier sense multiple access (CSMA) regions. However, TDMA results in inefficient utilization of the shared medium, as only one user transmits at a time. To allow simultaneous transmissions in MIMO systems, the technique known as interference alignment (IA) has been proposed [6, Ch. 2]. By designing the precoding and combining matrices in a coordinated manner, such that the desired and interference signals are projected onto orthogonal spaces at the receiver side, the aggregate data rate of the network can be enhanced [7] [8] [9]. However, its feasibility is not always guaranteed and requires the number of streams to be lower than the number of degrees of freedom of the considered scenario. The latter is determined by the number of users, the number of transmitting and receiving ports, and the spatial correlation of the involved MIMO channels [6, Ch. 4].

The feasibility of IA in simplified PLC networks and under the assumption of uncorrelated noise between ports was assessed in [10]. These results were further extended in [11], showing that accounting for the spatial correlation (between ports) of PLC noise in the design of the precoding and combining matrices reported notable data rate gains.

Spatial correlation of PLC noise is particularly prominent in the 88–108 MHz band, where radiated frequency modulation (FM) emissions from broadcast services couple to all the conductors of the power lines in a similar way. The work in [12] showed that the exploitation of this phenomenon by means of a whitening transformation makes MIMO PLC feasible in the 88–108 MHz band, even if the power spectral density (PSD) of the injected signal is as low as -100 dBm/Hz.

The aim of this work is to evaluate the performance improvement achieved through the joint application of IA and noise whitening (NW) to indoor broadband MIMO PLC systems. In this context, it makes two main contributions:

- The assessment of the feasibility of IA strategies over conventional TDMA schemes in actual PLC channel frequency responses (CFRs) and noise registers measured in several European countries.
- The evaluation of the data rate gain achieved by combining IA and NW. The latter technique renders the equivalent channel non-reciprocal, as the noise differs between the transmitting and receiving ends. This degrades the performance of the most widely used IA algorithms, which assume channel reciprocity. To address this issue, a simple algorithm that does not rely on this premise is proposed. The assessment takes into account the overhead

of the feedback of the channel state information (CSI) required by the IA scheme.

The rest of the paper is organized as follows. Section II describes the system model. The employed IA algorithms are introduced in Section III and their performance is evaluated in Section IV. Finally, Section V concludes the paper.

II. System Model

Let us consider the multi-user interference scenario portrayed in Fig. 1, with N_u users sharing the same transmission media. Half of the users are configured as transmitters, and their indices are in the set $\mathcal{T}$. The other half are configured as receivers, and their indices are in the set $\mathcal{R}$. Each transmitter $j \in \mathcal{T}$ has a single target receiver, that is denoted as $r_j \in \mathcal{R}$. Likewise, each receiver $i \in \mathcal{R}$ has a single legitimate transmitter, that is denoted as $k_i \in \mathcal{T}$. This mutual relation can be expressed as $i = r_j \Leftrightarrow j = k_i \; \forall (i,j) : i \in \mathcal{R} \wedge j \in \mathcal{T}$. All users communicate simultaneously, so every receiver suffers interference coming from $N_\text{u}/2 - 1$ interfering transmitters. Each user employs an $N_\text{T} \times N_\text{R}$ MIMO OFDM system to convey N_str data streams.

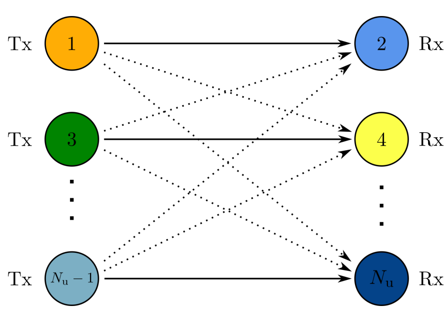

Fig. 1. Indoor PLC network with N_u users, half as transmitters and the other as receivers. There is only one legitimate transmitter for each receiver. Interfering links are drawn in dashed lines and legitimate ones in solid line. For illustrative purposes, odd indices are assigned to transmitters, $\mathcal{T} = \{1, 3, ..., N_\text{u} - 1\}$, and even indices to receivers, $\mathcal{R} = \{2, 4, ..., N_\text{u}\}$.

A. Transmission and Reception

Assuming that the cyclic prefix is long enough to avoid inter-symbol interference (ISI) and inter-carrier interference (ICI), the $N_\text{R} \times N_\text{T}$ MIMO CFR matrix between the j-th transmitter and the i-th receiver for the k-th subcarrier is denoted as $\mathbf{H}_{i,j}(k)$. For simplicity, expressions will be given for a generic subcarrier, so the index k will be omitted in the notation, i.e., $\mathbf{H}_{i,j}(k) = \mathbf{H}_{i,j}$.

Let $\mathbf{d}_j = [d_j^{(1)}, \ldots, d_j^{(N_\text{str})}]^\text{T}$ be the set of data symbols transmitted by the j-th user through all its data streams. These symbols are beamformed using the $N_\text{T} \times N_\text{str}$ matrix $\mathbf{V}_j$ and transmitted through the channel. The set of symbols received by the i-th user through all their ports can be expressed as

$$\mathbf{y}_i = [y_i^{(1)}, \ldots, y_i^{(N_\text{R})}]^\text{T} = \mathbf{H}_{i,k_i}\mathbf{V}_{k_i}\mathbf{d}_{k_i} + \sum_{j \in \mathcal{R}; j \neq i} \mathbf{H}_{i,k_j}\mathbf{V}_{k_j}\mathbf{d}_{k_j} + \mathbf{z}_i, \tag{1}$$

where $\mathbf{z}_i$ is the $N_\text{R} \times 1$ vector that contains the samples of noise present in the receiving ports, which is assumed to be zero mean. The streams are decoded from $\mathbf{y}_i$ using the $N_\text{R} \times N_\text{str}$ projection matrix $\mathbf{U}_i$. The l-th data stream received by user i, can be expressed as

$$s_i^{(l)} = \overbrace{(\mathbf{u}_i^{(l)})^\text{H}\mathbf{H}_{i,k_i}\mathbf{v}_{k_i}^{(l)}d_{k_i}^{(l)}}^{\hat{s}_i^{(l)}} + \overbrace{\sum_{(j,m) \neq (i,l)} (\mathbf{u}_i^{(l)})^\text{H}\mathbf{H}_{i,k_j}\mathbf{v}_{k_j}^{(m)}d_{k_j}^{(m)}}^{\check{s}_i^{(l)}}, \tag{2}$$

for all $i, j \in \mathcal{R}$ and for $l, m = 1, \ldots, N_\text{str}$, where $\mathbf{u}_i^{(l)}$ and $\mathbf{v}_{k_i}^{(m)}$ are the l-th and m-th columns of matrices $\mathbf{U}_i$ and $\mathbf{V}_{k_i}$, respectively, and $\hat{s}_i^{(l)}$, $\check{s}_i^{(l)}$ represent the desired and the interfering parts of the symbol, respectively. Interference comes from the data streams transmitted by other users and from other data streams from the legitimate user.

Assuming that the data symbols transmitted in each stream are white and independent of the sequences transmitted in other streams, and provided that $\mathbb{E}\left\{d_j^{(l)}(d_j^{(l)})^*\right\} = \rho_j^{(l)}$, where $\mathbb{E}\{\cdot\}$ denotes the expectation operator, the power of the desired signal in (2) is given by

$$P_{\hat{s}_i^{(l)}} = \mathbb{E}\left\{\hat{s}_i^{(l)}(\hat{s}_i^{(l)})^\text{H}\right\} = \rho_{k_i}^{(l)}(\mathbf{u}_i^{(l)})^\text{H}\mathbf{H}_{i,k_i}\mathbf{v}_{k_i}^{(l)}(\mathbf{v}_{k_i}^{(l)})^\text{H}\mathbf{H}_{i,k_i}^\text{H}\mathbf{u}_i^{(l)}, \tag{3}$$

and the one of the interfering signal, $P_{\check{s}_i^{(l)}} = \mathbb{E}\left\{\check{s}_i^{(l)}(\check{s}_i^{(l)})^\text{H}\right\}$, by

$$P_{\check{s}_i^{(l)}} = \sum_{(j,m) \neq (i,l)} \rho_{k_j}^{(m)}(\mathbf{u}_i^{(l)})^\text{H}\mathbf{H}_{i,k_j}\mathbf{v}_{k_j}^{(m)}(\mathbf{v}_{k_j}^{(m)})^\text{H}\mathbf{H}_{i,k_j}^\text{H}\mathbf{u}_i^{(l)}. \tag{4}$$

The expression of the signal to interference and noise ratio (SINR) for the l-th received data stream of the i-th user is

$$SINR_i^{(l)} = \frac{P_{\hat{s}_i^{(l)}}}{P_{\check{s}_i^{(l)}} + (\mathbf{u}_i^{(l)})^\text{H}\mathbf{\Phi}_i\mathbf{u}_i^{(l)}}, \tag{5}$$

where $\mathbf{\Phi}_i = \mathbb{E}\{\mathbf{z}_i\mathbf{z}_i^\text{H}\}$ is the noise correlation matrix at the receiver of the i-th user.

When NW is added to the considered system, the signal received by the i-th user, $\mathbf{y}_i$, is multiplied by a whitening matrix, $\mathbf{W}_i$, which is derived from $\mathbf{\Phi}_i$ [13, Sec. 9.2.1]. The presented analysis can still be applied just by considering that the effective channel between the i-th receiver and the j-th transmitter is $\widetilde{\mathbf{H}}_{i,j} = \mathbf{W}_i\mathbf{H}_{i,j}$, and the whitened noise, $\mathbf{w}_i = \mathbf{W}_i\mathbf{z}_i$, is spatially uncorrelated and has unitary power. It is worth noting that the resulting effective channel is no longer reciprocal, since the whitening matrix depends on the noise at the receiving side.

III. Interference Alignment Algorithms

This section describes the four IA iterative algorithms employed in this work. The first three algorithms are taken from the literature, while the fourth is proposed as an adaptation of one of the former to non-reciprocal scenarios.

A. IA algorithms reliant on channel reciprocity

Two widespread IA iterative algorithms for designing the precoding and combination matrices are the so-called Min-IL (minimize interference leakage) and Max-SINR (maximize

SINR) proposed in [7]. The first one seeks to minimize the interference at each receiver (disregarding the noise), and the second is aimed at maximizing the SINR of each data stream. By exploiting the channel reciprocity, both of them can be implemented in a distributed manner that requires only local system information. This avoids the need of exchanging CSI, however, a training phase is required for the receivers to learn the channel from their legitimate transmitter, and also the interference and noise statistics. This training phase must be performed at each iteration, which entails an important efficiency loss. In this work, we employ the extension of the Max-SINR algorithm made in [11] to account for the spatial correlation of noise between PLC receiving ports.

B. IA algorithms non-reliant on channel reciprocity

Since the NW procedure makes the equivalent channel non-reciprocal, the performance of the Min-IL and Max-SINR algorithms is unknown and their convergence is not guaranteed when combined with NW. To address this issue, two iterative algorithms that do not rely on this property are employed. They must be implemented in a centralized fashion and CSI from all users has to be available.

1) Generalized Min-IL (G-Min-IL): This iterative algorithm was proposed as a generalization of Min-IL that does not rely on channel reciprocity. The reader is kindly referred to [8] for further details.

2) Generalized Max-SINR (G-Max-SINR): We propose this algorithm as an adaptation of the Max-SINR in [11] to non-reciprocal scenarios. It aims at maximizing the SINR of all users simultaneously.

The interference plus noise correlation matrix for the i-th receiving user and the l-th data stream is computed as

$$\boldsymbol{\Upsilon}_i^{(l)} = \sum_{\substack{(j,m)\neq(i,l);\\ j\in\mathcal{R};\\ m\in\{1,\ldots,N_{\text{str}}\}}} \rho_{k_j}^{(m)} \mathbf{H}_{i,k_j} \mathbf{v}_{k_j}^{(m)} (\mathbf{v}_{k_j}^{(m)})^{\text{H}} \mathbf{H}_{i,k_j}^{\text{H}} + \boldsymbol{\Phi}_i. \quad (6)$$

Then, the columns of the combining matrix that maximize the SINR of the l-th data stream can be obtained as [7]

$$\mathbf{u}_i^{(l)} = \frac{\left(\boldsymbol{\Upsilon}_i^{(l)}\right)^{-1} \mathbf{H}_{i,k_i} \mathbf{v}_{k_i}^{(l)}}{\left\| \left(\boldsymbol{\Upsilon}_i^{(l)}\right)^{-1} \mathbf{H}_{i,k_i} \mathbf{v}_{k_i}^{(l)} \right\|}. \quad (7)$$

Since channel reciprocity does not hold, the following matrix is proposed to account for the interference that the l-th stream of user j produces in other streams,

$$\boldsymbol{\Psi}_j^{(l)} = \sum_{\substack{(i,m)\neq(r_j,l);\\ i\in\mathcal{R};\\ m\in\{1,\ldots,N_{\text{str}}\}}} \rho_j^{(m)} \mathbf{H}_{i,j}^{\text{T}} (\mathbf{u}_i^{(m)})^* (\mathbf{u}_i^{(m)})^{\text{T}} \mathbf{H}_{i,j}^* + \boldsymbol{\Phi}_{r_j}. \quad (8)$$

The columns of the precoding matrices that maximize the SINR are obtained as

$$\mathbf{v}_j^{(l)} = \frac{\left(\boldsymbol{\Psi}_j^{(l)}\right)^{-1} \mathbf{H}_{r_j,j}^{\text{T}} (\mathbf{u}_{r_j}^{(l)})^*}{\left\| \left(\boldsymbol{\Psi}_j^{(l)}\right)^{-1} \mathbf{H}_{r_j,j}^{\text{T}} (\mathbf{u}_{r_j}^{(l)})^* \right\|}. \quad (9)$$

The SINR after each iteration is then obtained using (5). These magnitudes are computed for every transmitter $j \in \mathcal{T}$, every receiver $i \in \mathcal{R}$ and for every stream $l \in \{1, \ldots, N_{\text{str}}\}$. These steps are repeated until the change in the SINR in subsequent iterations is lower than a given threshold.

IV. NUMERICAL RESULTS

This section assesses the performance attained by the presented IA algorithms with and without NW. The case in which interference between users is avoided by means of TDMA is used as a reference. The assessment is carried out using a set of 40 noise registers and 113 CFR matrices measured in Belgium, Germany and the United Kingdom [14]. These CFR and noise registers are randomly arranged to assemble 1000 multi-user scenarios, each with $N_{\text{u}} = 4$ users.

All users employ a 2×2 MIMO scheme, through which they transmit $N_{\text{str}} = 1$ data streams. The latter is determined by the feasibility condition [6], which limits the number of data streams per user to $N_{\text{str}} \leq (N_{\text{T}} + N_{\text{R}})/(N_{\text{u}}/2 + 1)$. In any other case, N_{str} depends on the multiplexing gain of the MIMO channel, but is limited to $N_{\text{str}} \leq \min\{N_{\text{R}}, N_{\text{T}}\}$.

An OFDM system like the one defined in the ITU-T G.hn is employed [3], except that the bandwidth is extended up to 108 MHz, but keeping the subcarrier spacing to $\Delta f = 24.41$ (kHz). Since measured CFRs are only available up to 100 MHz, values in the $100 - 108$ MHz band are estimated from the ones in the $92 - 100$ MHz range as $[\mathbf{H}_{i,j}(f)]_{p,q} = 10^{\alpha(f-100)/10}[\mathbf{H}_{i,j}(200 - f))]_{p,q}$, for $100 \leq f\,(\text{MHz}) \leq 108$ and α is introduced to account for the low pass profile of PLC channels and is computed from the robust regression fit of the attenuation of corresponding MIMO path, $[\mathbf{H}_{i,j}(f)]_{p,q}$, for $2 \leq f\,(\text{MHz}) \leq 100$. Pulses have raised cosine (RC) shaped transitions. As for the injected PSD, we follow the ITU Rec. G.9964 [15]. In the 88-108 MHz subband, the injected PSD is limited to -100 dBm/Hz to avoid interfering FM emissions. As a reference, it is worth mentioning that this value is lower than the limit imposed by the European Standard EN 50561-1 for the excluded frequency ranges defined to prevent PLC systems from interfering with existing radio services in the band below 30 MHz [16]. The spectral efficiency is limited to $b_{\text{max}} = 12$ bit/s/Hz.

All IA algorithms are iterated a maximum of 5000 times. They are considered to have converged if the optimization metric varies less than 10^{-12} between iterations.

As a figure of merit, the sum rate attained in each scenario is used,

$$S = \sum_{i\in\mathcal{R}} R_i, \quad (10)$$

where R_i is the data rate for the receiving user i. While the distribution of the noise and interference is unknown, assuming them to be Gaussian and independent to each other gives a lower bound for the bit rate, since the Gaussian distribution has the largest entropy for a given variance,

$$R_i = \Delta f \sum_{k\in\mathcal{K}} \sum_{l=1}^{N_{\text{str}}} \min\left\{b_{\text{max}}, \log_2\left(1 + SINR_i^{(\ell)}(k)\right)\right\}, \quad (11)$$

where $\mathcal{K}$ denotes the set of active carriers.

For the TDMA case, only one user transmits at a time. Hence, there is no interference from unwanted transmitters and the attainable sum rate for each user is $R_i^{\text{TDMA}} = R_i/(N_{\text{u}}/2)$, with R_i computed from (11) with $P_{\tilde{s}_i^{(l)}} = 0$.

A. Sum rate performance

The sum rate achieved with each of the IA algorithms, both on their own and in combination with NW, is obtained using (10) and their cumulative distribution function (CDF) is calculated. The sum rate for the TDMA system, with and without NW, is provided as a baseline. The case where NW is employed will be denoted as 'NW', while 'w/o NW' refers to the case in which it is not used. Since noise correlation is much higher in the $88-108$ MHz band, the analysis separately assesses the performance improvement given by NW in this band and in the $2-88$ MHz one.

1) 2–88 MHz subband: Fig. 2 (a) shows the CDF of the sum rate obtained in the frequency band 2–88 MHz when the four proposed algorithms, with and without combining it with the NW scheme, are evaluated in the 1000 PLC scenarios. A notable result is that the sum rate distribution for algorithms Min-IL and G-Min-IL is roughly the same regardless of whether NW is applied (the four curves almost overlap). This effect is due to both algorithms focusing exclusively on reducing the interference without accounting for the noise. At the same time, their distribution is similar to that of the sum rate attained by the TDMA. It is noted that NW yields losses when combined with Min-IL and, specially, Max-SINR. For the former, losses are minimal, while for the latter the 80th percentile value is degraded from 1.48 Gbit/s down to 1.21 Gbit/s. The reason is that they rely on channel reciprocity, which is lost when the noise is whitened. On the other hand, G-Max-SINR leverages the SINR gain resulting from spatial noise decorrelation and achieves an increase of 95.6 Mbit/s in the 20th percentile, and 50 Mbit/s in the 50th and 80th percentiles with respect to the IA 'w/o NW' system. It must be emphasized the notable sum rate improvement achieved by the combined IA and NW with respect to the TDMA case, which is 356 Mbit/s in the 50th percentile.

In order to assess the gain given by the combined use of IA and NW with respect to the case where IA is used without NW in each of the 1000 scenarios employed in the study, Fig. 2 (b) shows the CDF of the sum rate gain, defined as the ratio of the sum rates of both cases. As observed, the Max-SINR yields losses in almost 100% of the scenarios. Similarly, with Min-IL, 60% of the scenarios experience sum rate losses of up to 10% when NW is applied. Only in 10% of the scenarios gains greater than 5% are obtained. These losses are due to these algorithms relying on channel reciprocity, a condition that is lost due to NW.

Regarding the G-Min-IL and G-Max-SINR, it can be observed that they yield sum rate losses in certain scenarios, which may seem contradictory to the results shown in Fig. 2 (a), where curves corresponding to the combined use of IA and NW appear to the right of those corresponding to IA without NW. The CDF moves to the right when adding NW, even if the sum rate is degraded in some scenarios, because the sum rate is improved in most scenarios and the degraded sum rate values are still higher than those of other scenarios of the 'w/o NW' case. Nevertheless, adding NW yields almost no gains when G-Min-IL is used, which is due to this algorithm disregarding the noise. Interestingly, when G-Max-SINR is employed, sum rate gains greater than 11% are achieved in 20% of the scenarios, although sum rate losses of up to 5% occur in approximately 8% of the scenarios. Since Min-IL and Max-SINR have proved to be perform poorer than G-Min-IL and G-Max-SINR in non-reciprocal scenarios, in the following only the latter two will be considered.

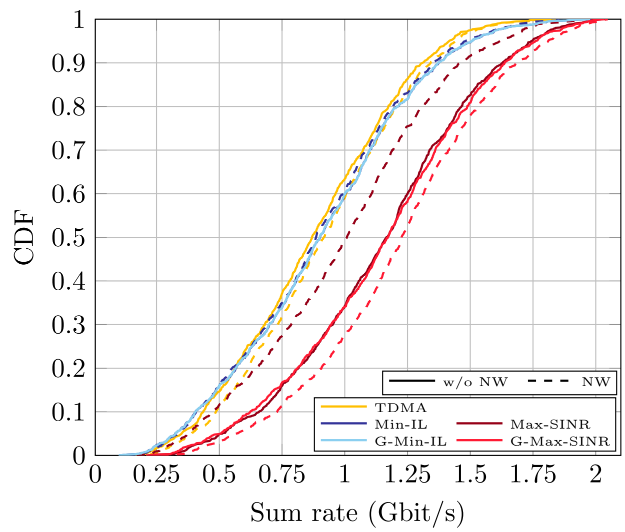

(a)

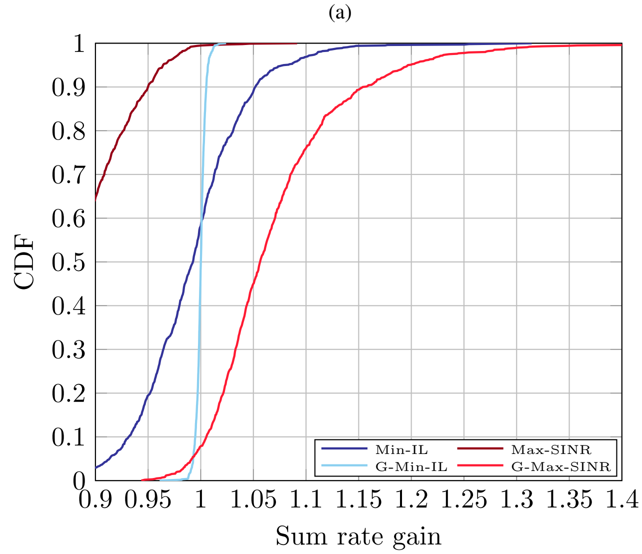

(b)

Fig. 2. CDF of the (a) sum rate of the TDMA, IA and combined IA and NW schemes; (b) sum rate gain of the combined IA and NW scheme with respect to the IA without NW in the 2–88 MHz frequency band.

2) 88–108 MHz subband: Fig. 3 (a) shows the CDF of the sum rate obtained in the 88–108 MHz subband. As seen, the median value of the attained sum rate is much lower than a quarter of the median in the 2–88 MHz band, despite the bandwidth of the 88–108 MHz range is one quarter of the former. This is due to the low PSD imposed to the injected signal, which is 15 dB lower than the one in the 30–88 MHz band. The dominance of noise over interference is such that decorrelating the noise generally gives higher sum rates than the ones achieved by eliminating the interference at the receiver. This is evinced by the G-Min-IL case (its two curves overlap), whose CDFs are to the left of the one of the TDMA with NW. Regarding G-Max-SINR, the improvement over the IA 'w/o NW' system is 8 Mbit/s at the median and 17 Mbit/s at the 80th percentile. Compared to the TDMA system, these values increase to 24 Mbit/s and 69.8 Mbit/s, respectively.

While these values are lower than those obtained in the 2–88 MHz, it must be taken into account that the reference bit rates are also lower. To assess the gain obtained in each channel, Fig. 3 (b) shows the CDF of the sum rate gain obtained by the combined use of IA and NW with respect to the IA without NW. As expected, the gain that NW gives when combined with G-Min-IL is limited and, in about half of the scenarios, is counterproductive. In contrast, when G-Max-SINR is used, the attainable gain exceeds 20% in 40% of the scenarios, and are greater than 36% in 20% of them.

B. *Overhead due to CSI feedback*

The proposed G-Min-IL and G-Max-SINR require the receiving nodes to transmit their CSI to a centralized entity that calculates the optimal precoding and receiving matrices. Then, the latter are transmitted to the corresponding nodes. The total number of coefficients exchanged between the central entity and the users in this process is

$$M_{\text{coef}} = (N_{\text{u}}/2 \cdot N_{\text{u}}/2 \cdot N_{\text{T}} \cdot N_{\text{R}} + N_{\text{u}}/2 \cdot N_{\text{R}}^2 + N_{\text{u}}/2 \cdot N_{\text{str}} \cdot N_{\text{T}} + N_{\text{u}}/2 \cdot N_{\text{str}} \cdot N_{\text{R}}) \cdot N_{\text{sc}}, \tag{12}$$

where N_{sc} denotes the number of active subcarriers.

The first and second addends between brackets on the right-hand side of (12) accounts for the initial CSI exchange (CFR and noise correlation matrices), and the second and third terms account for the transmission of the optimal IA matrices to the corresponding users. During the CSI exchange, each receiving user transmits to the central unit their estimates of the $N_{\text{T}} \times N_{\text{R}}$ sized CFR matrices with every other transmitting user. The noise correlation matrices are $N_{\text{R}} \times N_{\text{R}}$. After the optimal precoding ($N_{\text{T}} \times N_{\text{str}}$) and receiving ($N_{\text{R}} \times N_{\text{str}}$) matrices are computed, they are sent to the corresponding transmitters and receivers, respectively. This procedure is performed for every active subcarrier.

Provided that the PLC channel varies over time, the data rate required for the CSI exchange between users and the central unit can be obtained as $(2 \cdot M_{\text{coef}} \cdot B)/T_{\text{coh}}$, where the 2 accounts for the real and imaginary parts of each coefficient, B denotes the number of bits used to represent each coefficient and T_{coh} is the channel coherence time. Indoor PLC channels show short-term and long-term variations. For the moment, the former component will be neglected, for its effect to be

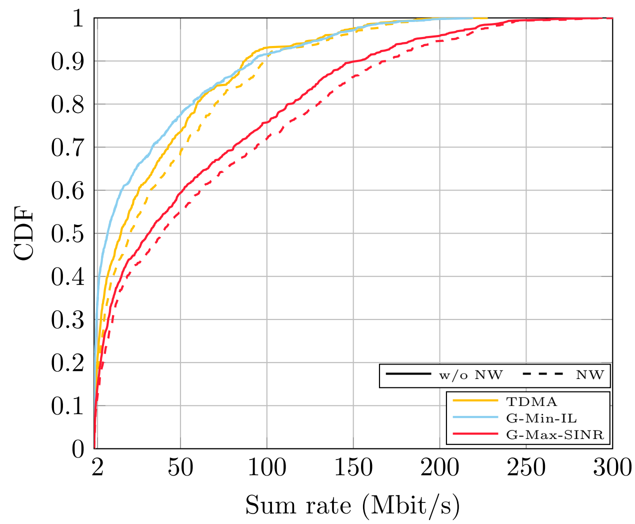

(a)

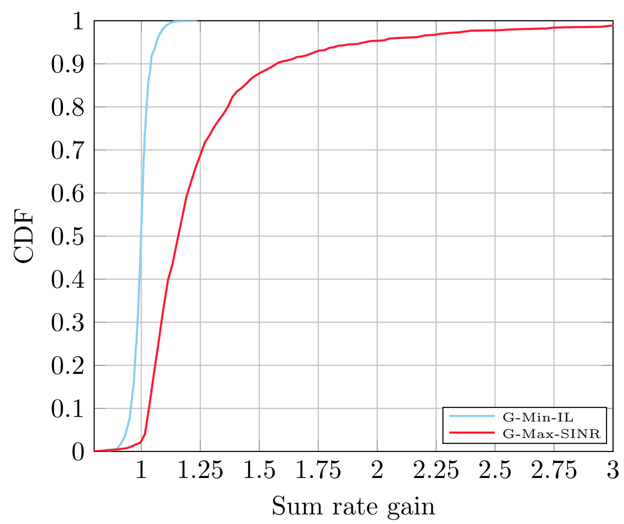

(b)

Fig. 3. CDF of the (a) sum rate of the TDMA, IA and combined IA and NW schemes; (b) sum rate gain of the combined IA and NW scheme with respect to the IA without NW in the 88–108 MHz frequency band.

studied thereafter. The long-term variations are produced by the connection and disconnection of devices from the grid, which can be assumed to occur every several minutes.

As a reference, the data rate required to exchange the CSI and IA matrices in the scenario proposed in the previous subsection is given in Table I. Two subbands are considered, 2–88 MHz and the 88–108 MHz, and two different coherence times are used: 4 minutes (240 s) and 10 minutes (600 s). It should be emphasized that, even in the wider subband, the data rate required to exchange these matrices is several orders of magnitude below the gain that the proposed scheme attains in most scenarios. For example, when considering the 2–88 MHz subband, the proposed scheme attains gains greater than 1% in 90% of the scenarios, since the base sum rate is 700 Mbit/s. This means that the sum rate increment is approximately 1000 times the data rate required for the CSI exchange. This can be alternatively interpreted as follows: reporting the CSI at the referred bit rate (707 Mbit/s) results in an efficiency loss of only 0.001%.

TABLE I
BIT RATE REQUIRED FOR THE CSI EXCHANGE PROCEDURE IN THE 2–88 MHZ AND THE 88–108 MHZ BANDS.

Subband	N_{sc}	B	T_{coh}	Bit rate
$2-88$ MHz	3522	16 bits	240 s	7.51 kbit/s
			600 s	3 kbit/s
$88-108$ MHz	819	16 bits	240 s	1.75 kbit/s
			600 s	0.7 kbit/s

If the short-term variations were to be accounted for, their periodic nature, synchronous with the mains frequency, allows for a simple solution: defining a few (4 or 8) regions within a cycle where the channel can be considered time-invariant, and obtaining the optimal IA matrices for those regions. This procedure entails multiplying the rates in Table I by the number of considered regions. However, this increase is still far outweighed by the attained gains.

V. CONCLUSION

This work has assessed the sum rate gain given by the combined use of IA and NW to improve the sum rate achieved in indoor broadband MIMO PLC multi-user scenarios. Since most IA algorithms have been derived under the assumption that the channel is reciprocal, a condition that no longer holds when NW is added, an iterative IA algorithm designed to operate without depending on this property has been proposed. Its performance has been assessed in a set of 1000 scenarios generated from measured CFR and noise registers.

The presented results indicate that the combined use of IA and NW enhances the sum rate of MIMO PLC multi-user scenarios, provided that the employed IA algorithm aims to maximize the SINR rather than merely create an interference-free subspace. The gain achieved by adding NW to the IA process is particularly beneficial in frequency bands where the dominant noise components are radio frequency interferences coupled to the power line conductors via radiation, such as in the 88–108 MHz band, where the proposed scheme attains a median sum rate of approximately 40 Mbit/s with an injected PSD of only -100 dBm/Hz. The addition of NW requires the IA process to be performed in a centralized manner. However, the resulting gains in sum rate have been shown to more than compensate for the overhead associated with CSI exchange.

ACKNOWLEDGMENT

The work of Javier Giménez, José A. Cortés and Luis Díez is funded in part by the Spanish Government under FPU grant FPU20/03782 and project PID2019-109842RB-I00/AEI/10.13039/501100011033, and by the Universidad de Málaga under project PAR 15/2023.

REFERENCES

[1] S. Aboagye, T. M. N. Ibrahim, A. Ngatched, A. R. Ndjiongue, and O. A. Dobre, “Design of energy efficient hybrid VLC/RF/PLC communication system for indoor networks,” *IEEE Wireless Communications Letters*, vol. 9, no. 1, pp. 143–147, Feb. 2020.

[2] K. Ali, A. X. Liu, I. Pefkianakis, and K. H. Kim, “Distributed spectrum sharing for enterprise powerline communication networks,” *IEEE/ACM Transactions on Networking*, vol. 29, no. 3, pp. 1032–1045, Jun. 2021.

[3] “Unified high-speed wireline-based home networking transceivers - System architecture and physical layer specification,” ITU-T Recommendation G.9960, July 2015.

[4] “Unified high-speed wireline-based home networking transceivers - multiple input/multiple output specification,” ITU-T Recommendation G.9963, December 2011.

[5] “HomePlug AV Specification Version 2.1,” HomePlug Alliance, Specification. [Online]. Available: https://bit.ly/39YvjXB, Feb. 2014.

[6] S. Jafar, *Interference Alignment: A New Look at Signal Dimensions in a Communication Network*. Now Publishers Inc., 2011. [Online]. Available: https://books.google.es/books?id=GfwB7ItK4esC

[7] K. Gomadam, V. R. Cadambe, and S. A. Jafar, “A distributed numerical approach to interference alignment and applications to wireless interference networks,” *IEEE Trans. on Inf. Theory*, vol. 57, no. 6, pp. 3309–3322, 2011.

[8] S. W. Peters and R. W. Heath, “Interference alignment via alternating minimization,” in *2009 IEEE Int. Conf. on Acoust., Speech and Signal Process.*, 2009, pp. 2445–2448.

[9] ——, “Cooperative algorithms for MIMO interference channels,” *IEEE Trans. on Veh. Technol.*, vol. 60, no. 1, pp. 206–218, 2011.

[10] M. J. Rahman and L. Lampe, “Interference alignment for MIMO power line communications,” in *IEEE Int. Symp. on Power Line Commun. and Its Appl. (ISPLC)*, 2015, pp. 71–76.

[11] ——, “On noise correlation in interference alignment for MIMO power line communications,” in *IEEE Global Commun. Conf. (GLOBECOM)*, 2019, pp. 1–5.

[12] J. A. Cortés, J. A. Corchado, F. J. Cañete, and L. Díez, “Analysis and exploitation of the noise correlation in MIMO power line communications in the FM band,” *IEEE Commun. Lett.*, vol. 22, no. 3, pp. 566–569, 2018.

[13] L. T. Berger, A. Schwager, P. Pagani, and D. M. Scheneider, Eds., *MIMO Power line Communications: Narrow and Broadband Standards, EMC and Avanced Processing*, 1st ed. Boca Raton, FL: CRC Press, 2014.

[14] ETSI, “PowerLine Telecommunications (PLT). MIMO PLT. Part 3: Setup and Statistical Results of MIMO PLT Channel and Noise Measurements,” *TR 101 562-3 V1.1.1 (2012-02)*, 2012.

[15] “Unified high-speed wireline-based home networking transceivers - Power spectral density specification,” ITU-T Recommendation G.9964, December 2011.

[16] “Power line communication apparatus used in low-voltage installations - Radio disturbance characteristics - Limits and methods of measurement - Part 1: Apparatus for in-home use,” European Standard, EN 50561-1, October 2013.